Journal of the Serbian Chemical Society
JSCS-info@shd.org.rs • www.shd.org.rs/JSCS
J. Serb. Chem. Soc. *84* (8) 891–900 (2019) UDC 546.11–12+66.091:539.196:532.14:548.7
JSCS–5232 *Original scientific paper*

Hydrogen transfer reaction: Bond formation and bond cleavage through the eyes of interacting quantum atoms

BRANISLAV Ž. MILOVANOVIĆ[#], MIHAJLO R. ETINSKI and MILENA M. PETKOVIĆ[#]*

Faculty of Physical Chemistry, University of Belgrade, Studentski trg 12–16, PAC 105305, 11158 Belgrade, Serbia

(Received 26 February, accepted 6 May 2019)

Abstract: Hydrogen transfer from hydroquinone to the methoxy radical was studied using the density functional theory. The energy decomposition technique, interacting quantum atoms, was employed for a detailed investigation of the changes that the bonds of interest go through along the minimum energy path in the vicinity of the transition state. The whole system was divided either into two or three fragments. The two-fragment analysis enabled investigation of the bond that is formed or the one that is cleaved by defining the fragments as reactants and as products, respectively. The three-fragment analysis (the fragments being semiquinone, hydrogen atom and methoxy radical) was used for the simultaneous analysis of the two phenomena, bond cleavage and bond formation. Additionally, it enabled the interaction between the particle that donates the hydrogen atom and the one that accepts it to be investigated. This interaction is characterized by attractive non-classical and repulsive classical interactions. It was demonstrated that the transferring hydrogen atom undergoes the most pronounced energy changes and gives the largest contribution to the deformation energy.

Keywords: interacting quantum atoms; density functional theory; antioxidants; polyphenols; radicals.

INTRODUCTION

Due to their importance in living organisms, scavenging properties of numerous antioxidants have been extensively investigated both by experimentalists and theoreticians.[1–7] Most of such investigations focused on the determination of the rate constants for the analyzed reactions,[8,9] the theoretical estimation of which rests on precise determination of barrier heights.[10–12]

Polyphenols are well-known as efficient antioxidants.[13,10] Recently, the reactions between the smallest representative of polyphenols, hydroquinone, and

*Corresponding author. E.mail: milena@ffh.bg.ac.rs
[#] Serbian Chemical Society member.
https://doi.org/10.2298/JSC190226034M

the hydroxyl/hydroperoxyl radical were analyzed.[14] The mechanism of the formal hydrogen transfer and the sequence the two species (the proton and the electron) are transferred were studied. In a subsequent paper,[15] hydrogen transfer from hydroquinone to the methoxy radical was investigated by employing the interacting quantum atoms methodology to obtain a deeper insight into the energy changes that accompany this reaction. In the current contribution, the analysis of the same system, hydroquinone (HQ) and the methoxy radical (Me$^\bullet$), is continued with the focus on the properties of the two O–H bonds that play a crucial role in this hydrogen transfer reaction, *i.e.*, the one that is broken O(HQ)–H and the one that is formed O(Me)–H. More precisely, the energy components of the two bonds along the intrinsic reaction path in the vicinity of the transition state are analyzed by employing interacting quantum atoms methodology, which has hitherto been widely used for the investigation of interactions between fragments in various systems.[16–23]

COMPUTATIONAL PROCEDURE

All calculations were performed at the uM06-2X/6-31+G(d,p) level[24-28] with the Gaussian program package[29] using an ultrafine integration grid. It has already been shown that the M06-2X functional successfully describes numerous systems,[30,31] including open shell systems such as organic radicals.[32] Optimization of the stationary points was performed with tight convergence criteria. The optimized transition state is characterized with a single imaginary frequency. The intrinsic reaction coordinate (IRC) calculations confirmed that the optimized first order saddle point connects the species of interest: the hydrogen bonded complexes of the reactants HQ···Me$^\bullet$ and the hydrogen bonded complex of the products HQ$^\bullet$···Me. IRC was performed by employing the Hessian-based predictor-corrector integrator.[33-35]

The energy decomposition analysis was performed using the interacting quantum atoms (IQA) method. The interaction energy between two fragments (interacting particles) that form a complex (a supermolecule) was computed along the IRC in the reactant and in the product valley close to the transition state.

The IQA methodology rests on the Bader theory of atoms in molecules[36] according to which the total space is divided into subspaces, each belonging to a certain atom. Pendás and co-workers extended Bader's idea to the IQA[37] methodology, and its variant interacting quantum fragments procedure[38] (for simplicity, the abbreviation IQA will be used for the interacting quantum fragments methodology, which is employed in this manuscript). The interaction energy, E(IQA), between two fragments F_1 and F_2 is represented as the sum of four terms:

$$E(\mathrm{IQA}) = E_{\mathrm{cl}} + E_{\mathrm{xc}} + E_{\mathrm{def}}(\mathrm{F_1}) + E_{\mathrm{def}}(\mathrm{F_2}) \quad (1)$$

where E_{cl} and E_{xc} stand for the classical and the non-classical energy component, respectively. E_{def} represents the deformation energy estimated by subtracting fragment's energy in vacuum at its geometry in the complex from the corresponding value in a supermolecule. The IQA analysis was performed with the AIMAll program package.[39] The Promega5 basin integration method insured small deviation of the IQA energy from the density functional theory (DFT) values (the largest discrepancy amounted to 3 kJ mol^{-1}). The reported charges are the Bader's charges computed with the AIMAll program.

RESULTS AND DISCUSSION

As mentioned in the Introduction, the reaction between hydroquinone and the methoxy radical:[15] HQ···Me$^{\bullet}$ → HQ$^{\bullet}$···Me, has recently been analyzed. Both the reactants and the products are hydrogen bonded and hence, this reaction could be viewed as transformation of the reactant complex into the product complex. Two transition states were reported that differ in the orientation of the reactants.[15] Although the corresponding barrier heights differ by only 2 kJ mol^{-1} and the two mechanisms are thus equally probable, it was demonstrated that the energy components obtained according to the interacting quantum atoms (IQA) methodology substantially differ. In the current contribution, the focus was on the description of the system in the vicinity of the slightly more stable transition state by applying the interacting quantum fragments methodology not just at the transition state but also on non-stationary points. Such analysis was previously employed for the investigation of nucleophilic substitution in α-haloketones describing the whole transformation of the reactants into products.[40] Herein, the focus is on a small fragment of intrinsic reaction coordinate (IRC) around the transition state. For a detailed analysis, the first ten points starting from the first-order saddle point in the reverse and in the forward direction will be considered. This segment of the IRC will be named as the segment of interest. According to the geometric properties,[15] the transition state resembles the reactant complex, Fig. 1. This is also the case in hydrogen transfer reactions from hydroquinone to the hydroxyl and the hydroperoxyl radical.[14] Consequently, energy changes in the segment of interest are much more pronounced in the product valley, Fig. 2A. The difference in O(HQ)–H and O(Me)–H bond lengths along the IRC are depicted in Fig. 2B. In accord with the above discussion, this value is positive at the TS.

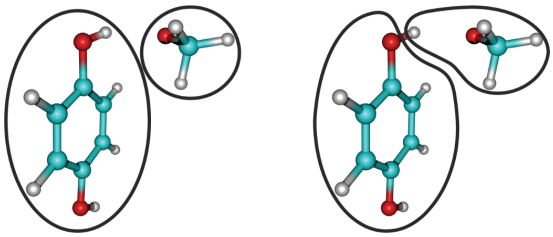

Fig 1. Transition state for hydrogen transfer from hydroquinone to the methoxy radical. The chosen fragments are HQ and Me$^{\bullet}$ (left) or HQ$^{\bullet}$ and Me (right).

First, what is meant by fragments needs to be defined. One would assume HQ and Me$^{\bullet}$ to represent fragments until the top of the barrier, and HQ$^{\bullet}$ and Me beyond the saddle point. In the former case, information about the O(Me)–H bond would be obtained and in the latter, about the O(HQ)–H bond. In order to describe changes in both O–H bonds, both representations in the vicinity of the transition state in the whole segment of interest must be considered.

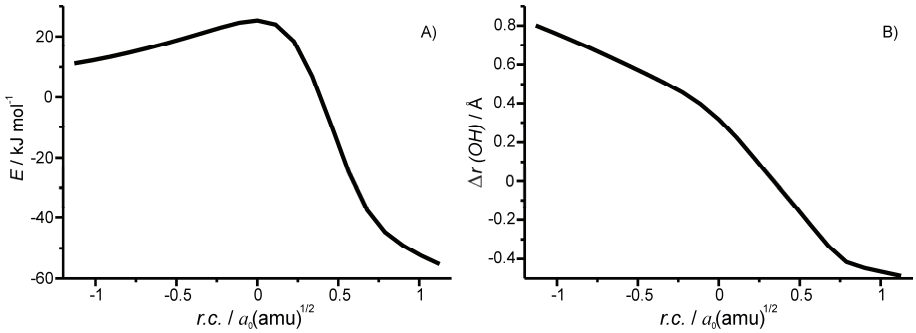

Fig. 2. Change of electronic energy (A) and difference in O(Me)–H and O(HQ) bond lengths (B) along the intrinsic reaction path in the vicinity of the transition state.

This discussion will contribute to gain a deeper understanding of the properties of the two bonds, the one being broken and the one being formed.

First, the focus will be on interaction energy between HQ and Me•. The results of the IQA analysis are presented in Fig. 3A. *E*(IQA) displays very small changes in the reactant valley, but significantly decreases beyond the transition state. Both the classical and the non-classical interaction energy have negative values with the latter being dominant in the reactant valley. They have almost the same values around $0.5a_0(\text{amu})^{1/2}$ and the classical term becomes more negative beyond this point. The deformation energy of HQ significantly rises upon hydrogen detachment. It reaches a maximum around $0.5a_0(\text{amu})^{1/2}$ and slightly decreases thereafter. E_{def}(Me) is also characterized with positive values, although considerably lower compared to its counterpart.

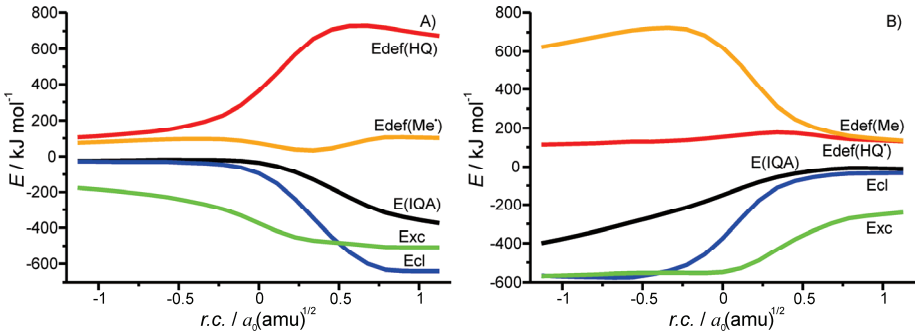

Fig. 3. Energy changes along the reaction coordinate when the fragments are: A) HQ & Me• and B) HQ• & Me.

Now, let the same system be analyzed from another perspective. Since this reaction might proceed in the opposite direction, the interacting fragments could be defined as HQ• and Me. The corresponding IQA energy components are displayed in Fig. 3B. As the reaction advances, the IQA energy and both interaction

terms become less negative. The classical and the non-classical interaction part have comparable contribution of around $-1.0a_0(\text{amu})^{1/2}$, whereas the exchange--correlation term is more pronounced in the product valley. The deformation energy terms are positive with noticeably large values for Me in the reactant valley. The presented results indicate the covalent character of the O(HQ)–H bond and clearly demonstrate its weakening as the reaction advances.

Note that the energy terms presented in Fig. 3A and B roughly represent mirror images of each other. An energy decrease accompanies the formation of the O(Me)–H bond, whereas the increase in the interaction energy characterizes cleavage of the O(HQ)–H bond. Particular energy components display the same trend. Concerning the deformation energy in the HQ & Me$^\bullet$ system, hydroquinone is substantially disturbed upon hydrogen detachment. On the other hand, in the HQ$^\bullet$ & Me system, deformation energy of methanol is very large as long as the hydrogen atom is bonded to O(HQ). Reaction advance is accompanied with decrease in both the classical and non-classical interaction energy in the HQ & Me$^\bullet$ pair, whereas their increase characterizes reaction progress considered through HQ$^\bullet$ & Me interaction.

Since the interaction energy terms according to IQA methodology contain only pair interactions, the whole system could be divided into three components: HQ$^\bullet$, Me$^\bullet$ and a hydrogen atom. Such analysis would enable the simultaneous investigation of both bonds of interest. To the best of our knowledge, this is the first application of interacting quantum fragments on more than two particles, *i.e.*, more than two fragments (note that interaction among more than two fragments has already been performed, for example see Ref. 41). The energy components describing HQ$^\bullet$/Me$^\bullet$ and H interaction are presented in Fig. 4A and B. Deformation energies of all three fragments are positive, with the hydrogen atom being significantly more disturbed than either of the other two species. Both the classical and the non-classical component of the inter-particle interaction become less negative upon bond cleavage and more negative as the bond is formed.

The interaction between HQ$^\bullet$ and Me$^\bullet$ is presented in Fig. 4C. Interestingly, slightly beyond the transition state, the deformation energies of the two particles can be viewed as mirror images of each other. This is also the case with the classical and the non-classical part of the interaction energy. Note that the classical interaction is repulsive. Finally, the overall energy changes are depicted in Fig. 4D. The deformation energy strongly destabilizes the whole system, but is overpowered by the total interaction energy between the three pairs of particles, resulting in the negative overall binding energy, the changes of which in the region of interest can hardly be noticed on this energy scale. Despite the positive E_{cl} values in Fig. 4C, classical interactions between the three pairs of fragments become more pronounced beyond $0.6a_0(\text{amu})^{1/2}$.

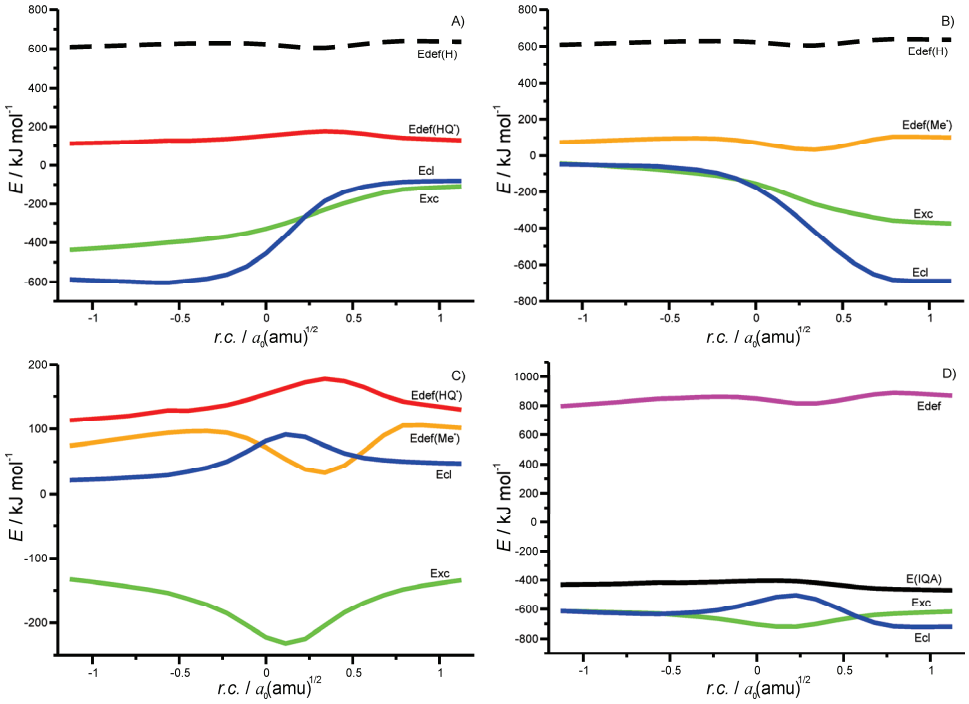

Fig. 4. Energy changes along the reaction coordinate when the fragments are HQ• & H & Me•. Interaction and deformation terms between: A) HQ• & H; B) Me• & H; C) HQ• & Me•; D) overall deformation energy and interaction energy.

Positive values of the classical interaction energy between HQ• and Me• prompted an examination of the charges of the three fragments. The results are presented in Fig. 5A. In the part of the region of interest where this energy term shows a maximum, the electron is being transferred from hydroquinone to the methoxy radical and at around $0.08a_0(\text{amu})^{1/2}$, the two particles have identical

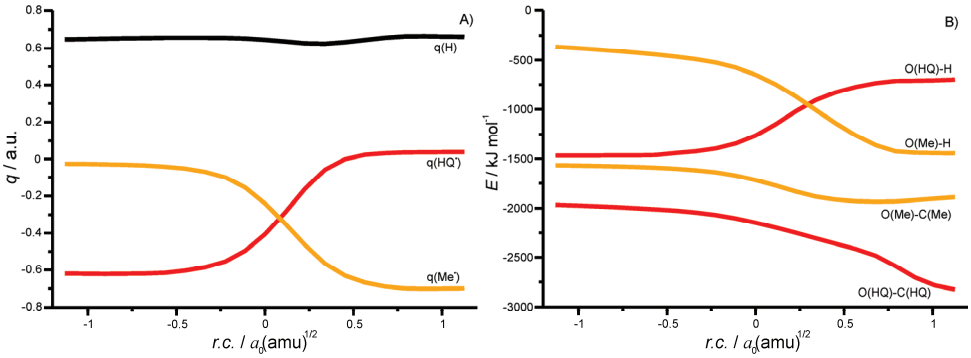

Fig. 5. A) The Bader charges of H, HQ• and Me•. B) Interaction energy among the atoms O(HQ) & H, O(Me) & H, O(HQ) & C(HQ) and O(Me) & C(Me).

charges of approximately –0.3 e. The fact that the charge of the hydrogen in the region of interest amounts to +0.65 e raises a question of whether it should be considered as a positive ion (a proton) instead of an atom. However, the charges of Me$^{\bullet}$ at the beginning of the segment of interest and of HQ$^{\bullet}$ at its end are close to zero, which is the reason why these two fragments were considered as neutral. Consequently, the charge of the hopping fragment was set to zero to keep the whole system uncharged.

Finally, the interaction energy between the hydrogen atom and the two oxygen atoms, Fig. 5B, will be examined. Both interactions are attractive and nicely demonstrate O(HQ)–H cleavage and O(Me)–H formation. These changes are reflected in interactions between oxygen atoms and their other neighbours, the carbon atoms. O(HQ)'s interaction with C(HQ) (the carbon atom in the aromatic ring) becomes significantly stronger, in accord with a transformation of a single bond into one with a partial double bond character. On the other hand, accumulation of the negative charge on O(Me) strengthens the O(Me)–C(Me) bond, although to a lesser extent.

CONCLUSIONS

Hydrogen transfer reactions represent a dominant mechanism in the deactivation of dangerous radical species. In the example discussed in this contribution, hydroquinone and methoxy radical, cleavage of O–H bond of the antioxidant is coupled to the formation of an O–H bond with the radical, which transforms it into a harmless (*i.e.*, non-reactive) molecule. In order to gain deeper insight into energy changes associated with the transformations of the two bonds, energy decomposition analysis was performed using the interacting quantum atoms approach. Since the very moment when the two bonds change their nature (from a covalent to a hydrogen bond and *vice versa*) was of interest, the part of the intrinsic reaction path in the vicinity of the transition state was analyzed in the direction of the reactants and in the direction of the products. The energy decomposition approach rests on computation of the interaction energy between the selected fragments. Defining the fragments as hydroquinone and methoxy radical allows analysis of the O(Me)–H bond, whereas interaction between semiquinone and methanol enables investigation of the O(HQ)–H bond. The presented results describe bond changes from the perspective of interacting quantum atoms, destabilization of the O(HQ)–H bond and stabilization of the O(Me)–H bond. It has been demonstrated that by appropriately choosing the fragments, energy decomposition methods could be successfully employed for analysis of bond cleavage and bond formation. Decomposition of the whole system into three particles allowed the simultaneous monitoring of O(HQ)–H cleavage and O(Me)–H formation.

Acknowledgements. The authors would like to express their gratitude to Prof. Miljenko Perić, to whose 70th birthday this issue of the *J. Serb. Chem. Soc.* is dedicated, for introducing

them the world of Quantum Chemistry and inspiring them to further explore it. Financial support is provided by the Ministry of Education, Science and Technological Development of the Republic of Serbia through Project No. 172040. Quantum chemical calculations were performed on the PARADOX cluster at the Scientific Computing Laboratory of the Institute of Physics, Belgrade, supported in part by the Serbian Ministry of Education, Science and Technological Development under Project No. ON171017.

ИЗВОД

РЕАКЦИЈА ПРЕНОСА АТОМА ВОДОНИКА: НАСТАНАК И КИДАЊЕ ВЕЗЕ СА АСПЕКТА ИНТЕРАГУЈУЋИХ КВАНТНИХ АТОМА

БРАНИСЛАВ Ж. МИЛОВАНОВИЋ, МИХАЈЛО Р. ЕТИНСКИ и МИЛЕНА. М. ПЕТКОВИЋ

Факултет за физичку хемију, Универзитет у Београду, Студентски трг 12–16, ПАК 105305, 11158 Београд

Пренос атома водоника са хидрохинона на метокси радикал анализиран је помоћу теорије функционала густине. Метода разлагања енергије на одговарајуће доприносе, интерагујући квантни атоми, коришћена је за детаљно испитивање промена кроз које пролазе две најбитније везе у овом процесу дуж пута минималне енергије у околини прелазног стања. Цео систем је подељен или на два, или на три фрагмента. Анализа заснована на два фрагмента је омогућила проучавање везе која настаје или везе која се кида, у зависности од тога да ли су фрагменти дефинисани као реактанти или као производи реакције. Анализа заснована на три фрагмента (при чему фрагменте представљају семихинон, атом водоника и метокси радикал) је коришћена за истовремену анализу оба феномена, настајање и кидање везе. Поред тога, омогућила је проучавање интеракције између даваоца и примаоца атома водоника. Ова интеракција је окарактерисана привлачним интеракцијама које не представљају Кулонове интеракције и одбојним класичним интеракцијама. Показано је да атом водоника који се преноси подлеже најизраженијим енергетским променама и даје највећи допринос деформационој енергији.

(Примљено 26. фебруара, прихваћено 6. маја 2019)

REFERENCES

1. M. Polovka, C. Brezová, A. Staško, *Biophys. Chem.* **106** (2003) 39 (https://doi.org/10.1016/S0301-4622(03)00159-5)
2. V. B. Luzhkov, *Chem. Phys.* **314** (2005) 211 (https://doi.org/10.1016/j.chemphys.2005.03.001)
3. T. L. Duarte, J. Lunec, *Free Radic. Res.* **39** (2005) 671 (https://doi.org/10.1080/10715760500104025)
4. S. Fiorucci, J. Golebiowski, D. Cabrol-Bass, S. Antonczak, *J. Agric. Food Chem.* **55** (2007) 903 (https://doi.org/10.1021/jf061864s)
5. A. Karadag, B. Ozcelik, S. Saner, *Food Anal. Method.* **2** (2009) 41 (https://doi.org/10.1007/s12161-008-9067-7)
6. K. Sadasivam, R. Kumaresan, *Mol. Phys.* **109** (2011) 839 (https://doi.org/10.1080/00268976.2011.556576)
7. M. Carocho, I. C. F. R. Ferreira, *Food Chem. Toxicol.* **51** (2013) 15 (https://doi.org/10.1016/j.fct.2012.09.021)
8. Y. Kono, K. Kobayashi, S. Tagawa, K. Adachi, A. Ueda, Y. Sawa, H. Shibata, *Biochim. Biophys. Acta* **1335** (1997) 335 (https://doi.org/10.1016/S0304-4165(96)00151-1)
9. Y. Sueishi, M. Hori, M. Ishikawa, K. Matsuura, E. Kamogawa, Y. Honda, M. Kita, K. Ohara, *J. Clin. Biochem. Nutr.* **54** (2014) 67 (https://doi.org/10.3164/jcbn.13-53)

10. F. di Meo, V. Lemaur, J. Cornil, R. Lazzaroni, J.-L. Duroux, Y. Olivier, P. Trouillas, *J. Phys. Chem., A* **117** (2013) 2082 (https://doi.org/10.1021/jp3116319)
11. L. Muños-Rugeles, J. R. Alvarez-Idaboy, *Phys. Chem. Chem. Phys.* **17** (2015) 28525 (https://doi.org/10.1039/C5CP05090A)
12. L. Muñoz-Rugeles, A. Galano, J. R. Alvarez-Idaboy, *Phys. Chem. Chem. Phys.* **19** (2017) 15296 (https://doi.org/10.1039/C7CP01557G)
13. W. Bors, C. Michel, *Ann. N. Y. Acad. Sci*. **957** (2002) 57 (https://doi.org/10.1111/j.1749-6632.2002.tb02905.x)
14. Đ. Nakarada, M. Petković, *Int. J. Quant. Chem.* **118** (2018) e25496 (https://doi.org/10.1002/qua.25496)
15. M. Petković, Đ. Nakarada, M. Etinski, *J. Comp. Chem.* **39** (2018) 1868 (https://doi.org/10.1002/jcc.25359)
16. O. A. Syzgantseva, V. Tognetti, L. Houbert, *J. Phys. Chem., A* **117** (2013) 8969 (https://doi.org/10.1021/jp4059774)
17. Z. Badri, C. Foroutan-Nejad, J. Kozelka, R. Marek, *Phys. Chem. Chem. Phys.* **17** (2015) 26183 (https://doi.org/ 10.1039/C5CP04489H)
18. I. Cukrowski, P. Mangondo, *J. Comput. Chem.* **37** (2016) 1373 (https://doi.org/10.1002/jcc.24346)
19. J. Jara-Cortés, B. Landeros-Rivera, J. Hernándes-Trujillo, *Phys. Chem. Chem. Phys.* **20** (2018) 27558 (https://doi.org/10.1039/C8CP03775B)
20. T. A. N. Nguyen, G. Frenking, *Chem. Eur. J.* **18** (2012) 12733 (https://doi.org/10.1002/chem.201200741)
21. F. Zaccaria, G. Paragi, C. F. Guerra, *Phys. Chem. Chem. Phys.* **18** (2016) 20895 (https://doi.org/10.1039/C6CP01030J)
22. K. F. Andriani, G. Heinzelmann, G. F. Caramori, *J. Phys. Chem., B* **123** (2019) 457 (https://doi.org/10.1021/acs.jpcb.8b11287)
23. P. Jerabek, P. Schwerdtfeger, G. Frenking, *J. Comp. Chem.* **40** (2019) 247 (https://doi.org/10.1002/jcc.25584)
24. Y. Zhao, D. G. Truhlar, *Theor. Chem. Acc.* **120** (2008) 215 (https://doi.org/10.1007/s00214-007-0310-x)
25. A. D. McLean, G. S. Chandler, *J. Chem. Phys.* **72** (1980) 5639 (https://doi.org/10.1063/1.438980)
26. R. Krishnan, J. S. Binkley, R. Seeger, J. A. Pople, *J. Chem. Phys.* **72** (1980) 650 (https://doi.org/10.1063/1.438955)
27. T. Clark, J. Chandrasekhar, G. W. Spitznagel, P. v. R. Schleyer, *J. Comp. Chem.* **4** (1983) 294 (https://doi.org/10.1002/jcc.540040303)
28. M. J. Frisch, J. A. Pople, J. S. Binkley, *J. Chem. Phys.* **80** (1984) 3265 (https://doi.org/10.1063/1.447079)
29. *Gaussian 09, Revision D.01*, Gaussian Inc., Wallingford CT, 2009 (http://gaussian.com)
30. Y. Zhao, D. G. Truhlar, *Chem. Phys. Lett.* **502** (2011) 1 (https://doi.org/10.1016/j.cplett.2010.11.060)
31. Y. Zhao, D. G. Truhlar, *J. Chem. Theory Comput.* **7** (2011) 669 (https://doi.org/10.1021/ct1006604)
32. Y. Zhao, D. G. Truhlar, *J. Phys. Chem., A* **112** (2008) 1096 (https://doi.org/10.1021/jp7109127)
33. H. P. Hratchian, H. B. Schlegel, *J. Chem. Phys.* **120** (2004) 9918 (https://doi.org/10.1063/1.1724823)

34. H. P. Hratchian, H. B. Schlegel, *Theory and Applications of Computational Chemistry: The First 40 Years*, C. E. Dykstra, G. Frenking, K. S. Kim, G. Scuseria, Eds., Elsevier, Amsterdam, 2005, p. 195 (ISBN 9780080456249)
35. H. P. Hratchian, H. B. Schlegel, *J. Chem. Theory Comput.* **1** (2005) 61 (https://doi.org/10.1021/ct0499783)
36. R. F. W. Bader, *Atoms in Molecules: A Quantum Theory*; Oxford University Press, Oxford, 1990
37. M. A. Blanco, A. M. Pendás, E. Francisco, *J. Chem. Theory Comput.* **1** (2005) 1096 (https://doi.org/10.1021/ct0501093)
38. A. M. Pendás, M. A. Blanco, E. Francisco, *J. Comp. Chem.* **28** (2007) 161 (https://doi.org/10.1002/jcc.20469)
39. AIMAll (Version 17.11.14), T. A. Keith, T. K. Gristmill Software, Overland Park, KS, 2017 (http://aim.tkgristmill.com)
40. C. J. van der Westhuizen, *Ms. Thesis*, University of Pretoria, Pretoria, 2017 (http://hdl.handle.net/2263/63346)
41. M. Stojanović, M. Baranac-Stojanović, *Eur. J. Org. Chem.* **2018** (2018) 6230 (https://doi.org/10.1002/ejoc.201801047).